Sciencexpress Reports

Light-induced collective pseudospin precession resonating with Higgs mode in a superconductor

Ryusuke Matsunaga,[1]* Naoto Tsuji,[1] Hiroyuki Fujita,[1] Arata Sugioka,[1] Kazumasa Makise,[2] Yoshinori Uzawa,[3]† Hirotaka Terai,[2] Zhen Wang,[2]‡ Hideo Aoki,[1,4] Ryo Shimano[1,5]*

[1]Department of Physics, The University of Tokyo, Hongo, Tokyo, 113-0033, Japan. [2]Kobe Advanced Research Center, National Institute of Information and Communications Technology, Hyogo, 651-2492, Japan. [3]National Astronomical Observatory of Japan, Osawa, Mitaka, Tokyo 181-8588, Japan. [4]High Energy Accelerator Research Organization (KEK), Tsukuba, Ibaraki 305-0801, Japan. [5]Cryogenic Research Center, The University of Tokyo, Yayoi, Tokyo, 113-0032, Japan.

*Corresponding author. E-mail: matsunaga@thz.phys.s.u-tokyo.ac.jp (R.M.) shimano@phys.s.u-tokyo.ac.jp (R.S.)

†Present address: Terahertz Technology Research Center, National Institute of Information and Communications Technology, Tokyo, 184-8795, Japan.

‡Present address: Shanghai Institute of Microsystem and Information Technology, Chinese Academy of Sciences, Shanghai 200050, China.

Superconductors host collective modes that can be manipulated with light. We show that strong terahertz light field can induce oscillations of the superconducting order parameter in NbN with twice the frequency of the terahertz field. The result can be captured as a collective precession of Anderson's pseudospins in ac driving fields. A resonance between the field and the Higgs amplitude mode of the superconductor then results in large terahertz third-harmonic generation. The method we present here paves a way toward nonlinear quantum optics in superconductors with driving the pseudospins collectively, and can be potentially extended to exotic superconductors for shedding light on the character of order parameters and their coupling to other degrees of freedom.

Macroscopic quantum phenomena such as superconductivity and superfluidity emerge in a variety of physical systems such as metals, liquid helium, ultracold atomic quantum gases, and neutron stars. One manifestation of the macroscopic quantum nature is the appearance of characteristic collective excitations. Indeed, phenomena associated with collective modes such as second sound and spin waves in condensates have been revealed in superfluid helium (*1*, *2*) and in ultracold atomic gases (*3*, *4*).

Generally, collective modes in ordered phases arising from spontaneous symmetry breaking are classified into (i) gapless phase modes (Nambu-Goldstone (NG) mode) and (ii) gapped amplitude modes (Higgs mode) (*5*–*7*). In charged-particle systems such as superconductors with long-range Coulomb interactions, the gapless NG mode becomes massive, i.e., its energy is elevated to the plasma frequency as a result of the coupling to the gauge boson (photon field), which is referred to as the Anderson-Higgs mechanism (*8*, *9*). The Higgs amplitude mode in superconductors has been also studied theoretically (*6*, *10*–*15*);because it is not accompanied by charge fluctuations, it does not couple directly to electromagnetic fields in the linear response regime. This is why the Higgs mode in conventional *s*-wave superconductors was observed only recently after a nonadiabatic excitation with a monocycle terahertz (THz) pulse (*16*); previous observations were in a special case where the superconductivity coexists with charge density wave that makes the Higgs mode Raman-active (*17*, *18*). Hence many questions regarding the Higgs mode in superconductors remain unresolved: How does the mode couple to strong electromagnetic fields in nonlinear regime? Is it possible to dynamically control the Higgs mode and therefore the superconducting order parameter?

Recent advances in the intense THz generation technique (*19*, *20*) opens a new avenue for studying matter phases in non-equilibrium conditions. Amplitude- and phase-resolved spectroscopy using multi THz pulses has been realized (*21*), enabling the study of coherent transients in many-body systems in low energy range. Purpose of the present work is to explore coherent nonlinear interplay between collective mode in a superconductor and THz light field by investigating the real-time evolution of the order parameter under the driving field of a multi-cycle (as opposed to monocycle) THz pulse.

In order to study evolutions on picosecond time scale, we performed THz pump-THz probe spectroscopy (*16*, *22*) (Fig. 1A). To generate an intense multi-cycle THz pulse as a coherent driving source, we first created an intense monocycle THz pulse by the tilted-pulse front method with a $LiNbO_3$ crystal (*19*, *23*). The monocycle pulse then goes through a band-pass filter to produce a narrow-spectrum multi-cycle pulse. Three band-pass filters are used to generate the different center frequencies at 0.3, 0.6, or 0.8 THz, respectively, with their power spectra displayed in Fig. 1B. These photon energies are all below the superconducting gap of our NbN sample in the low temperature limit, which is 1.3 THz (Fig. 1C); this implies that the pump pulse does not generate quasiparticles (QPs) in one-photon processes at low temperatures. The sample is an *s*-wave superconductor NbN thin film with 24-nm thickness grown on an MgO substrate (*24*) with T_c=15 K. The ultrafast dynamics of the superconducting order parameter driven by the multi-cycle pump pulse is then probed through the transmittance of a monocycle THz pulse that enters the sample collinearly with the pump pulse with a variable time delay. In general, we can detect the temporal waveform of the transmitted probe THz electric field E_{probe} by varying the time delay of another optical gate pulse and using the electro-optic (EO) sampling method. In this experiment, we fix the timing of the optical gate pulse such that, in the absence of the pump, E_{probe} at this timing monotonically changes with temperature, reflecting the change of the order parameter. Temporal evolution of the order parameter induced by the THz pump is sensitively monitored through the change of E_{probe} relative to its value in the absence of the pump as a function of the pump-probe delay time t_{pp} (*16*, *22*); we denote this change as δE_{probe}. For details, see (*25*). Note that, in the present case, we could investigate the order parameter dynamics in the presence of coherently oscillating multi-cycle pump fields. The temporal waveform of the pump THz electric field E_{pump} is displayed in Fig. 1D for the center frequency of ω=0.6 THz and the maximum electric field of 3.5 kV/cm. Figure 1E shows δE_{probe} with t_{pp} at T=14-15.5 K, at which ω is greater than $2\Delta(T)$. In this temperature range, the probe electric field gradually increases as a function of t_{pp} to reach an asymptotic value, which indicates a reduction of the order parameter resulting from QP excitations (*22*). By contrast, at temperatures below 13 K where $2\Delta(T)$ exceeds ω (Fig. 1F), the long-term reduction of the order parameter be-

comes less prominent as temperature decreases, because the QP excitation is suppressed. We can immediately notice that an oscillatory signal emerges with a frequency 1.2 THz (=2ω) during the pump pulse irradiation, which indicates that the order parameter oscillates with twice the frequency of the driving field.

We can physically capture the 2ω oscillation of the order parameter in terms of the precession of Anderson's pseudospins (*26*). In the BCS ground state, two electrons with wavenumbers $\boldsymbol{k}$ and $-\boldsymbol{k}$ form a spin-singlet Cooper pair, with the BCS wavefunction given by

$$|\Psi_{\mathrm{BCS}}\rangle = \prod_{\mathbf{k}} \left(u_{\mathbf{k}} |00\rangle_{\mathbf{k}} + v_{\mathbf{k}} |11\rangle_{\mathbf{k}} \right), \quad (1)$$

where $|00\rangle_{\mathbf{k}}$ ($|11\rangle_{\mathbf{k}}$) denotes unoccupied (occupied) $\boldsymbol{k}$ and $-\boldsymbol{k}$. In Anderson's pseudospin formalism, the states $|11\rangle_{\boldsymbol{k}}$ and $|00\rangle_{\boldsymbol{k}}$ are represented by up and down pseudospins, respectively (*25*), where the BCS ground state is thought of as a quantum superposition of up and down pseudospins with amplitudes $v_{\boldsymbol{k}}$ and $u_{\boldsymbol{k}}$ for each $\boldsymbol{k}$, respectively (Fig. 2A). Note that the normal state has the pseudospins all up for $|\boldsymbol{k}| < k_{\mathrm{F}}$ and all down for $|\boldsymbol{k}| > k_{\mathrm{F}}$ at T=0 (Fig. 2B), where k_{F} is the Fermi wave number. Within this representation, the BCS Hamiltonian simply reads $H_{\mathrm{BCS}} = 2\sum_{\boldsymbol{k}} \mathbf{b}_{\boldsymbol{k}} \cdot \boldsymbol{\sigma}_{\boldsymbol{k}}$, where $\boldsymbol{\sigma}_{\boldsymbol{k}} = (\sigma_{\boldsymbol{k}}^{x}, \sigma_{\boldsymbol{k}}^{y}, \sigma_{\boldsymbol{k}}^{z})$ is the Anderson's pseudospin (*26*) mapped onto the Bloch sphere (Fig. 2C), while $\boldsymbol{b}_{\boldsymbol{k}}$=(-Δ', -Δ", $\varepsilon_{\boldsymbol{k}}$) is a pseudomagnetic field acting on $\boldsymbol{\sigma}_{\boldsymbol{k}}$. Here $\varepsilon_{\boldsymbol{k}}$ is the band dispersion measured from the Fermi energy, $\Delta = \Delta' + i\Delta'' = U\sum_{\boldsymbol{k}} \left(\sigma_{\boldsymbol{k}}^{x} + i\sigma_{\boldsymbol{k}}^{y} \right)$ is the complex order parameter, and U(>0) the pairing interaction. In equilibrium, each pseudospin is aligned along the pseudomagnetic field. The time evolution of the BCS state is then described by the Bloch equation for the pseudospins,

$$\frac{\partial}{\partial t}\boldsymbol{\sigma}_{\boldsymbol{k}} = 2\boldsymbol{b}_{\boldsymbol{k}} \times \boldsymbol{\sigma}_{\boldsymbol{k}}, \quad (2)$$

i.e., the time evolution of the BCS state is represented as the motion of the pseudospins in the pseudomagnetic field. For a spatially-homogeneous monochromatic electric field $\boldsymbol{E}\exp(i\omega t)$ irradiated onto a superconductor, the z component of $\boldsymbol{b}_{\boldsymbol{k}}$, in the nonlinear response regime, becomes (*25*)

$$\begin{aligned} \frac{\varepsilon_{\mathbf{k}-e\mathbf{A}(t)} + \varepsilon_{\mathbf{k}+e\mathbf{A}(t)}}{2} &= \varepsilon_{\mathbf{k}} + \frac{e^2}{2}\sum_{i,j} \frac{\partial^2 \varepsilon_{\mathbf{k}}}{\partial k_i \partial k_j} A_i(t) A_j(t) + O(A^4) \\ &= \varepsilon_{\mathbf{k}} - \frac{e^2}{2}\sum_{i,j} \frac{\partial^2 \varepsilon_{\mathbf{k}}}{\partial k_i \partial k_j} \frac{E_i E_j}{\omega^2} \exp(i2\omega t) + O(A^4), \end{aligned} \quad (3)$$

where $\boldsymbol{A}(t)$ is the vector potential representing the electric field. We can see that the leading term in the energy variation is $\sim \boldsymbol{A}(t)^2$, which is intuitively because electrons with charge $-e$ hybridize with holes with charge $+e$ in the condensed pair, leading to a nonlinear coupling between light and the condensate, and to the pseudospin precession with the frequency 2ω. The coherent collective precession of the pseudospins (Fig. 2D) manifests itself macroscopically as the order parameter oscillation, and the change of the order parameter in turn affects the pseudomagnetic field. We calculated the time evolution of the order parameter self-consistently by numerically solving the Bloch equation for the multi-cycle pulse (see (*25*) for details). The simulation indeed exhibits the order parameter oscillation with twice the frequency of the external electric field (Fig. 2E).

An analytic solution for the linearized Bloch equation can in fact be obtained (*27*), where the temporal variation of the order parameter amplitude [$\Delta(t) = \Delta + \delta\Delta(t)$] turns out to behave around 2ω=2Δ as

$$\delta\Delta(t) \propto \frac{1}{|2\omega - 2\Delta|^{1/2}} \cos(2\omega t - \varphi), \quad (4)$$

with ϕ being a phase shift that depends on ω. The divergence of the amplitude at 2ω=2Δ can be interpreted as a resonance between the induced pseudospin precession with frequency 2ω and the collective amplitude mode of the order parameter, namely the Higgs mode (*16*), with frequency 2Δ. We can then relate the nonlinear current density $\boldsymbol{j}_{\mathrm{NL}}$ induced by the external ac field with the change in the order parameter $\delta\Delta(t)$ via (*25*) as

$$\boldsymbol{j}_{\mathrm{NL}}(t) \propto \frac{e^2\Delta}{U} \boldsymbol{A}(t)\delta\Delta(t), \quad (5)$$

which takes a form of the London equation. This enables us to regard the nonlinear current, which reflects the dynamics of the order parameter, as a part of the supercurrent.

Because the coherent interaction between the superconductor and the THz electromagnetic radiation results in the nonlinear (2ω, 4ω, 6ω…) oscillations of the order parameter (Eq. 3), the nonlinear current in Eq. 5 should accommodate higher odd-order harmonics in the transmitted pump THz pulse. To confirm this, we have performed a nonlinear transmission experiments for the pump THz pulse (without the probe pulse) (Fig. 3A). Figure 3B shows the waveforms of the transmitted pump THz pulse above (15.5 K) and below (10 K) T_{c}=15 K; the waveform of the transmitted pulse below T_{c} is considerably distorted. The power spectra of the transmitted pump THz pulse are shown in Fig. 3C on a logarithmic scale and in Fig. 3D on an expanded linear scale at various temperatures. Below T=13 K, a prominent peak appears around 1.8 THz, which indeed coincides with 3ω. The intensity at 3ω as a function of the pump electric field strength, depicted in Fig, 3E on a log-log scale, obeys $|E_{\mathrm{pump}}|^6$ dependence, endorsing that the signal arises from the third harmonic generation (THG). The THG intensity at 10 K normalized by that of the incident pump pulse reaches 8×10^{-5}, which is high for a film with only 24-nm thickness and 3.5-kV/cm peak electric field (*28*). We can increase the interaction length up to about 0.2 μm, the penetration depth of the sample at 0.6 THz (*29*), which would result in even higher conversion efficiency. A shift of THG peak energy with temperature is discerned in Fig. 3D, which is attributed to the softening of the Higgs mode (2Δ(T)) toward T_{c}. The THG signal disappears before the softening completes because the resonant enhancement is rapidly suppressed when Δ(T) moves out of the narrow bandwidth of the incident pump field.

The 2ω oscillation of the order parameter and the THG are also observed for ω=0.3 and 0.8 THz pumping. Figure 4B summarizes the temperature dependence of the THG intensities for all of ω=0.3, 0.6, and 0.8 THz. For ω=0.3 and 0.6 THz, the THG signal peaks at 13.5 K and 10 K, respectively, whereas the THG signal for ω=0.8 THz monotonically increases with decreasing temperature. Comparing the temperature dependence of the order parameter 2Δ(T) (Fig. 4A) with twice the pump frequency 2ω (=0.6, 1.2, and 1.6 THz), one can deduce that the peak in the THG does fall upon 2ω=2Δ(T). The THG intensity in Eq. 5 depends on the change of the order parameter amplitude, which is resonantly enhanced when 2ω approaches the inherent Higgs amplitude mode 2Δ(T). Indeed, the temperature dependence of the THG intensity calculated with Eq. 5 shown in Fig. 4C agrees qualitatively with experiment in Fig. 4B. We conclude that the resonance of the Anderson's pseudospin precession in the superconductor is achieved by irradiation of THz pump, which results in large THG. We can note that the theoretical results in Fig. 4C exhibit sharp resonance peaks, which results from the lifetime of the Higgs mode assumed to be infinite (i.e., power-law decay) within the BCS approximation (*10*, *12*). In contrast, the observed resonance widths in Fig. 4B are finite, which may be caused by decaying channels for the Higgs mode and the finite spectral width of the pump pulse (Fig. 1B). There are in fact various possible decay processes, including scattering with single-particle excitations, impurities, phonons, or low-frequency NG mode that emerges near T_{c} (*30*), for which systematic studies are desirable (*31*).

We finally note that superconductors are known to exhibit highly nonlinear responses near the critical field or temperature, giving rise to nonlinear *I-V* characteristics and higher-order harmonics in transport

measurements with a frequency range from a few hertz to microwave (*32*–*34*). By contrast, the large nonlinear optical effect revealed here originates from resonance of ac fields to the collective amplitude mode of the order parameter, which leads to the strong THG emission in THz frequency range.

The time-resolved observation of the THz higher-order harmonics will provide a unique avenue for probing ultrafast dynamics of the order parameter in out-of-equilibrium superconductors. It is highly intriguing to explore the quantum trajectories of the pseudospins on Bloch sphere in the non-perturbative light-matter interaction regime with much higher THz fields, which would result in a dynamics of superconducting order parameter not attained in conventional regimes. The present scheme utilizing the nonlinear coupling between pseudospins and light can be also extended to unconventional superconductors such as the cuprate or iron-pnictide, which would provide new insight about the high-T_c superconductivity and the interplay between the superconducting phase and other coexisting/competing orders.

References and Notes

1. For a review, see e.g., A. J. Leggett, *Rev. Mod. Phys.* **47**, 331 (1975).
2. W. P. Halperin, L. P. Pitaevskii, Eds, *Helium III, Modern Problems in Condensed Matter Physics* (North-Holland, Amsterdam, 1990).
3. L. A. Sidorenkov, M. K. Tey, R. Grimm, Y. H. Hou, L. Pitaevskii, S. Stringari, Second sound and the superfluid fraction in a Fermi gas with resonant interactions. *Nature* **498**, 78–81 (2013). Medline doi:10.1038/nature12136
4. J. S. Krauser, U. Ebling, N. Fläschner, J. Heinze, K. Sengstock, M. Lewenstein, A. Eckardt, C. Becker, Giant spin oscillations in an ultracold Fermi sea. *Science* **343**, 157–160 (2014). Medline doi:10.1126/science.1244059
5. Y. Nambu, Axial Vector Current Conservation in Weak Interactions. *Phys. Rev. Lett.* **4**, 380–382 (1960). doi:10.1103/PhysRevLett.4.380
6. C. M. Varma, *J. Low Temp. Phys.* **126**, 901–909 (2002). doi:10.1023/A:1013890507658
7. G. E. Volovik, M. A. Zubkov, Higgs Bosons in Particle Physics and in Condensed Matter. *J. Low Temp. Phys.* **175**, 486–497 (2014). doi:10.1007/s10909-013-0905-7
8. P. W. Anderson, Plasmons, Gauge Invariance, and Mass. *Phys. Rev.* **130**, 439–442 (1963). doi:10.1103/PhysRev.130.439
9. P. W. Higgs, Broken symmetries, massless particles and gauge fields. *Phys. Lett.* **12**, 132–133 (1964). doi:10.1016/0031-9163(64)91136-9
10. A. F. Volkov, S. M. Kogan, *Zh. Eksp. Teor. Fiz.* **65**, 2038 (1973) [*Sov. Phys. JETP* **38**, 1018 (1974)].
11. R. A. Barankov, L. S. Levitov, B. Z. Spivak, Collective Rabi oscillations and solitons in a time-dependent BCS pairing problem. *Phys. Rev. Lett.* **93**, 160401 (2004). Medline doi:10.1103/PhysRevLett.93.160401
12. E. A. Yuzbashyan, M. Dzero, Dynamical vanishing of the order parameter in a fermionic condensate. *Phys. Rev. Lett.* **96**, 230404 (2006). Medline doi:10.1103/PhysRevLett.96.230404
13. T. Papenkort, V. M. Axt, T. Kuhn, Coherent dynamics and pump-probe spectra of BCS superconductors. *Phys. Rev. B* **76**, 224522 (2007). doi:10.1103/PhysRevB.76.224522
14. N. Tsuji, M. Eckstein, P. Werner, Nonthermal antiferromagnetic order and nonequilibrium criticality in the Hubbard model. *Phys. Rev. Lett.* **110**, 136404 (2013). Medline doi:10.1103/PhysRevLett.110.136404
15. Y. Barlas, C. M. Varma, Amplitude or Higgs modes in *d*-wave superconductors. *Phys. Rev. B* **87**, 054503 (2013). doi:10.1103/PhysRevB.87.054503
16. R. Matsunaga, Y. I. Hamada, K. Makise, Y. Uzawa, H. Terai, Z. Wang, R. Shimano, Higgs amplitude mode in the BCS superconductors Nb1-xTi(x)N induced by terahertz pulse excitation. *Phys. Rev. Lett.* **111**, 057002 (2013). Medline doi:10.1103/PhysRevLett.111.057002
17. R. Sooryakumar, M. V. Klein, Raman Scattering by Superconducting-Gap Excitations and Their Coupling to Charge-Density Waves. *Phys. Rev. Lett.* **45**, 660–662 (1980). doi:10.1103/PhysRevLett.45.660
18. P. B. Littlewood, C. M. Varma, Gauge-Invariant Theory of the Dynamical Interaction of Charge Density Waves and Superconductivity. *Phys. Rev. Lett.* **47**, 811–814 (1981). doi:10.1103/PhysRevLett.47.811
19. J. Hebling, K.-L. Yeh, M. C. Hoffmann, B. Bartal, K. A. Nelson, Generation of high-power terahertz pulses by tilted-pulse-front excitation and their application possibilities. *J. Opt. Soc. Am. B* **25**, B6 (2008). doi:10.1364/JOSAB.25.0000B6
20. For a review, see e.g., T. Kampfrath, K. Tanaka, K. A. Nelson, Resonant and nonresonant control over matter and light by intense terahertz transients. *Nat. Photonics* **7**, 680–690 (2013). doi:10.1038/nphoton.2013.184
21. F. Junginger, B. Mayer, C. Schmidt, O. Schubert, S. Mährlein, A. Leitenstorfer, R. Huber, A. Pashkin, Nonperturbative interband response of a bulk InSb semiconductor driven off resonantly by terahertz electromagnetic few-cycle pulses. *Phys. Rev. Lett.* **109**, 147403 (2012). Medline doi:10.1103/PhysRevLett.109.147403
22. R. Matsunaga, R. Shimano, Nonequilibrium BCS state dynamics induced by intense terahertz pulses in a superconducting NbN film. *Phys. Rev. Lett.* **109**, 187002 (2012). Medline doi:10.1103/PhysRevLett.109.187002
23. R. Shimano, S. Watanabe, R. Matsunaga, Intense Terahertz Pulse-Induced Nonlinear Responses in Carbon Nanotubes. *J. Infrared. Milli. Terahz. Waves* **33**, 861–869 (2012). doi:10.1007/s10762-012-9914-x
24. K. Makise, H. Terai, M. Takeda, Y. Uzawa, Z. Wang, Characterization of NbTiN Thin Films Deposited on Various Substrates. *Appl. Supercond. IEEE Trans.* **21**, 139–142 (2011). doi:10.1109/TASC.2010.2088350
25. Supplementary Materials are availabe online.
26. P. W. Anderson, Random-Phase Approximation in the Theory of Superconductivity. *Phys. Rev.* **112**, 1900–1916 (1958). doi:10.1103/PhysRev.112.1900
27. N. Tsuji, H. Aoki, arXiv:1404.2711 [cond-mat.supr-con].
28. The conversion efficiency was estimated without compensating the frequency dependence of the EO-sampling detection coefficient for the 1mm-thick ZnTe crystal. The correction would make the conversion efficiency even higher.
29. A. Kawakami, Y. Uzawa, Z. Wang, Frequency dependence of penetration depth for epitaxial NbN thin films at 0.1–1.1 THz. *Physica C* **412**, 1455–1458 (2004). doi:10.1016/j.physc.2004.01.161
30. P. V. Carlson, A. M. Goldman, Propagating Order-Parameter Collective Modes in Superconducting Films. *Phys. Rev. Lett.* **34**, 11–15 (1974). doi:10.1103/PhysRevLett.34.11
31. Such a study may reveal the underlying coupling strength of the superconducting order parameter with other excitations; for the case of charge-density-wave system, see e.g., H. Schaefer, V. V. Kabanov, J. Demsar, Collective modes in quasi-one-dimensional charge-density wave systems probed by femtosecond time-resolved optical studies. *Phys. Rev. B* **89**, 045106 (2014). doi:10.1103/PhysRevB.89.045106
32. L. P. Gorkov, G. M. Eliashberg, *Zh. Eksp. Teor. Fiz.* **54**, 612 (1968) [*Sov. Phys. JETP* **27**, 328 (1968)].
33. J. C. Amato, W. L. McLean, Measurement of the Superconducting Order-Parameter Relaxation Time from Harmonic Generation. *Phys. Rev. Lett.* **37**, 930–933 (1976). doi:10.1103/PhysRevLett.37.930
34. O. Entin-Wohlman, Third-harmonic generation in dirty superconductors. *Phys. Rev. B* **18**, 4762–4767 (1978). doi:10.1103/PhysRevB.18.4762
35. W. Zimmermann, E. H. Brandt, M. Bauer, E. Seider, L. Genzel, Optical conductivity of BCS superconductors with arbitrary purity. *Physica C* **183**, 99–104 (1991). doi:10.1016/0921-4534(91)90771-P

Acknowledgments: This work was supported by a Grant-in-Aid for Scientific Research (Grants Nos. 25800175, 22244036, 20110005, 25104709, 25800192, and 26247057) and Advanced Photon Science Alliance by the Photon Frontier Network Program from MEXT.

Supplementary Materials

www.sciencemag.org/cgi/content/full/science.1254697/DC1
Materials and Methods
Supplementary Text
Figs. S1 to S3
References

11 April 2014; accepted 24 June 2014
Published online 10 July 2014
10.1126/science.1254697

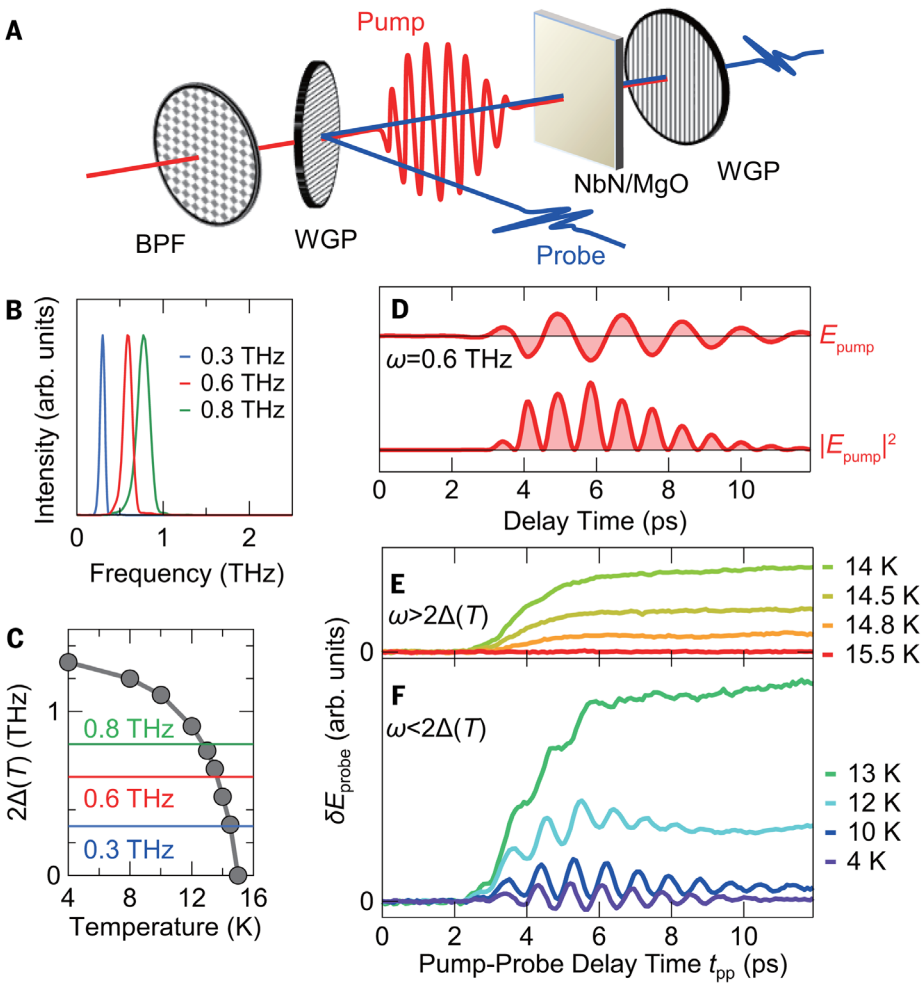

Fig. 1. THz pump-THz probe spectroscopy. (**A**) Schematic experimental setup for the THz pump-THz probe spectroscopy, where BPF is a metal-mesh band-pass filter and WGP a wire-grid polarizer. (**B**) Power spectra of the pump THz pulse with the center frequencies of ω=0.3, 0.6, and 0.8 THz. (**C**) Temperature dependence of the superconducting gap energy 2Δ of the NbN sample evaluated from the optical conductivity spectra based on the Mattis-Bardeen model (*35*). Horizontal lines indicate the center frequencies of the pump pulse. (**D**) Waveform of the pump THz electric field E_{pump} with the center frequency of ω=0.6 THz, with the squared $|E_{pump}|^2$ also shown. (**E**) The change in the probe THz electric field δE_{probe} as a function of the pump-probe delay time t_{pp} in the temperature range $2\Delta(T)<\omega$. Increase of δE_{probe} corresponds to a reduction of the order parameter. (**F**) δE_{probe} against t_{pp} in the temperature range $2\Delta(T)>\omega$.

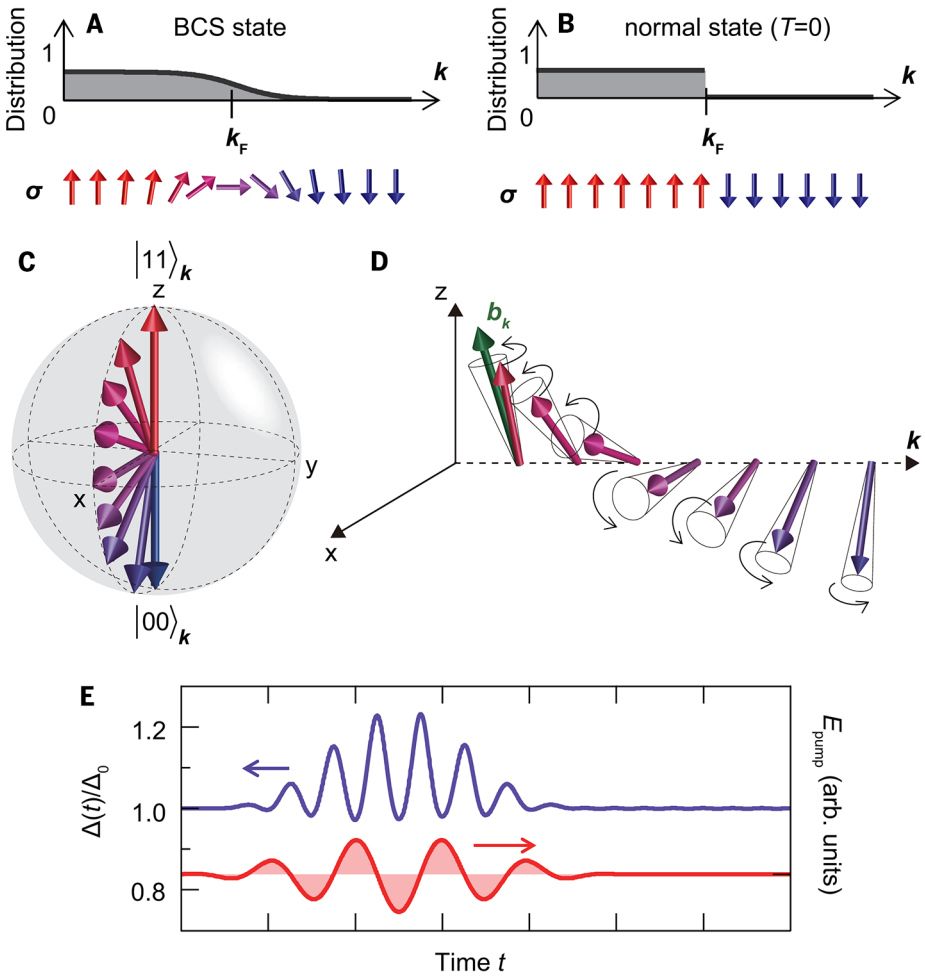

Fig. 2. Anderson's pseudospin model and simulation with Bloch equation. (**A, B**) Schematics of the electron distribution represented by Anderson's pseudospins for the normal state at T=0 and for the BCS state, respectively. (**C**) The pseudospins mapped on the Bloch sphere. (**D**) A schematic picture of the pseudospin precession. (**E**) Simulation of the Bloch equation showing the temporal evolution of the order parameter in an electric field (for details see (*25*)).

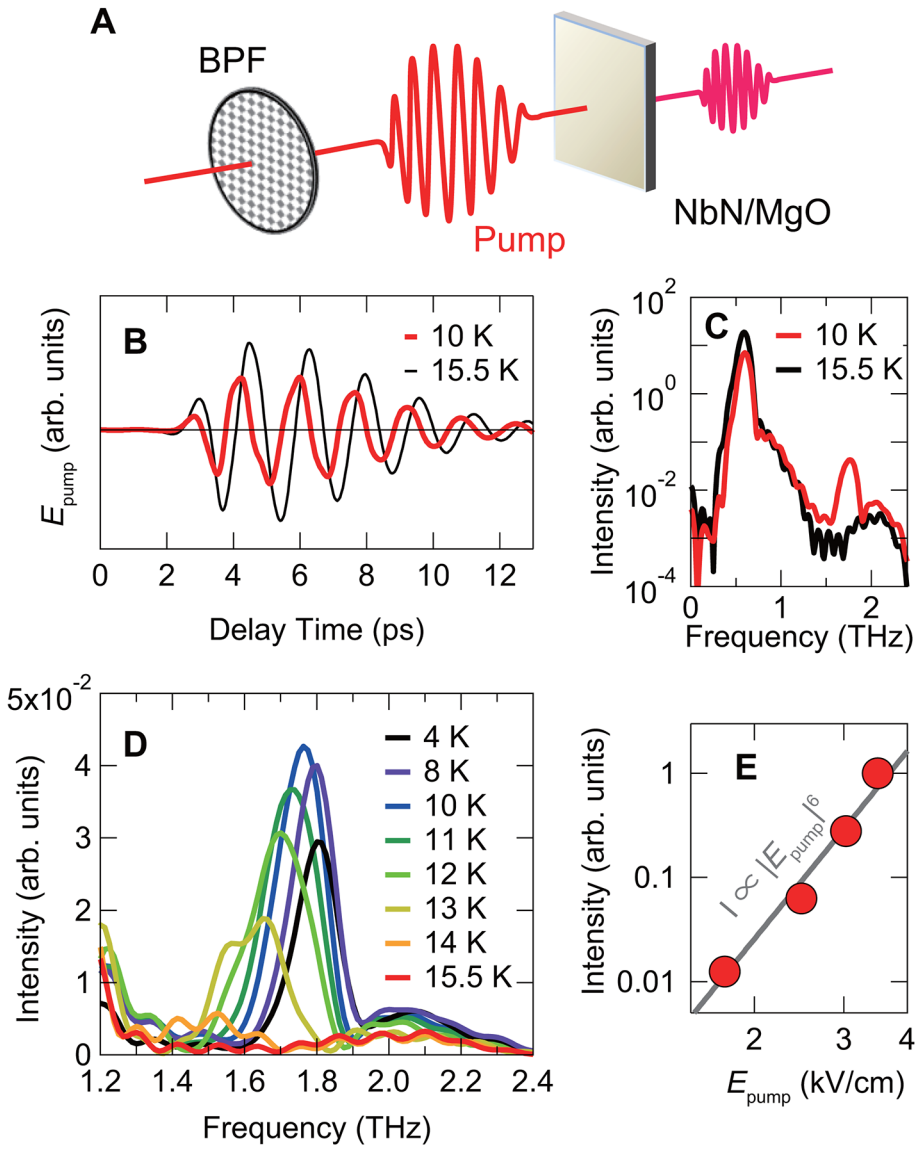

Fig. 3. THG in transmission spectroscopy. (**A**) A schematic of the nonlinear THz transmission experiment. (**B**, **C**) Waveforms and power spectra of the transmitted pump THz pulses below (10 K) and above (15.5 K) T_c=15 K, respectively. (**D**) Power spectra of the transmitted pump THz pulse at various temperatures. (**E**) THG intensity as a function of the pump THz field strength.

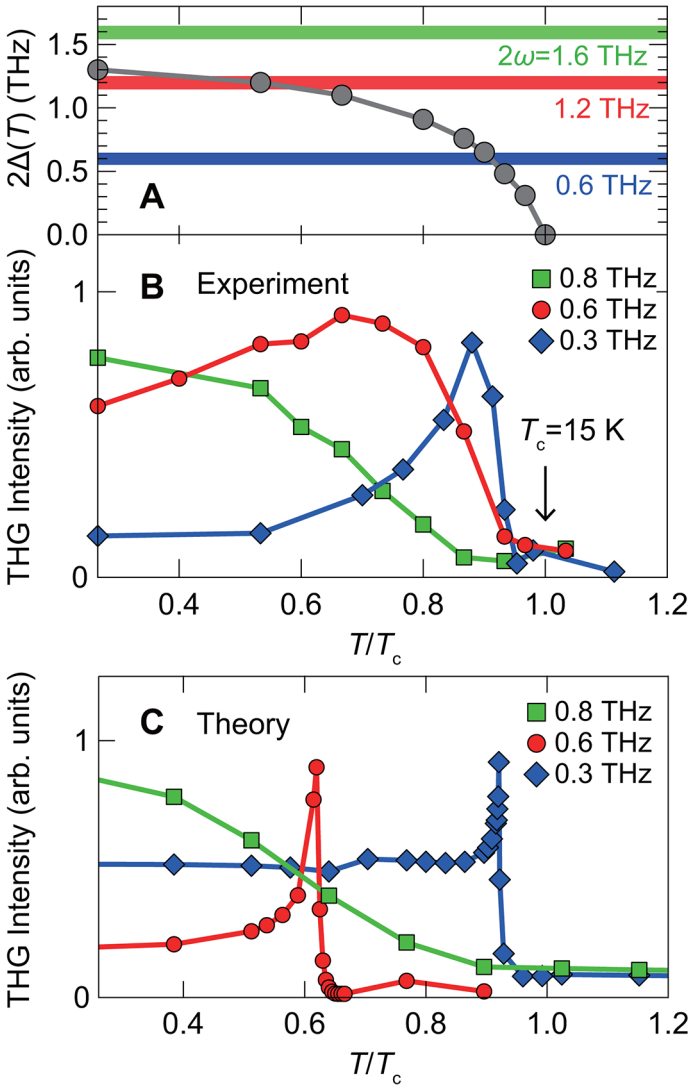

Fig. 4. Temperature dependence of the THG intensity. (**A**) Temperature dependence of the order parameter 2Δ(*T*) compared with twice the pump frequencies 2ω (horizontal lines). (**B**) Measured temperature dependence of the THG intensities at ω=0.3, 0.6 and 0.8 THz. (**C**) Calculated THG intensities as a function of temperature obtained by numerically solving the Bloch equation.